

Interaction between soft magnetic and superconducting films

Lars Egil Helseth

Max Planck Institute of Colloids and Interfaces, D-14424, Potsdam, Germany

Abstract

We study theoretically the interaction between soft magnetic and superconducting films. It is shown that the vortex induces a magnetization distribution in the magnetic film, thus modifying the magnetic field as well as the interactions with e.g. Bloch walls. In particular, the field from the vortex may change sign close to the core as a result of the vortex-induced magnetization, thus resulting in a crossover from attraction to repulsion between vortices and Bloch walls. Moreover, we show that by tuning the anisotropy field of the magnetic film, one may enhance the interaction between Bloch walls and vortices. Finally, we discuss how the structure of a Bloch wall in presence of the thin film superconductor can be revealed by magneto-optic imaging using an additional magneto-optic indicator.

I. INTRODUCTION

For centuries humans have tried to visualize magnetic fields using a variety of different devices. Iron particles, magnetic bacterias, Hall probes, ferro fluids, inductive coils, Lorentz microscopy and electron holography are just a few of these approaches. The last decades this research has been highly motivated by the need to visualize magnetic fields from superconductors. To this end, magneto-optic methods have proven particularly useful. In 1957 P.B. Abers visualized for the first time the magnetic field distribution from a superconductor using cerous nitrate glycerol[1]. A successful development followed in 1968, when Kirchner noted that chalcogenide films can be used to visualize these fields with improved sensitivity[2]. The next two decades magneto-optic imaging studies were published periodically, mostly concentrating on large scale flux penetration[3]. A major discovery was done in the beginning of the 1990's, when it was found that bismuth-substituted ferrite garnet films with in-plane magnetization are excellent indicators with very little domain activity (see e.g. Ref. [4]). This discovery triggered a large number of quantitative investigations of the flux behavior in high temperature superconductors, magnetic defects and phase transitions, microelectronic circuits and magnetic storage media [5, 6, 7, 8, 9, 10, 11, 12, 13]. Recently the long standing goal of imaging single vortices was achieved [14, 15]. This achievement opens a new dimension in the study of interactions between superconductors and soft magnetic films, and the first experimental results have already been obtained [6]. However, to date no theory exists which can explain future experimental results in this field. A key question here is how the vortices interact with the soft magnetic films, in particular with micromagnetic elements such as Bloch walls. To this end, it should be pointed out that several theoretical studies have been concerned with the interaction between vortices and magnetic nanostructures (see e.g. Ref. [17, 18, 19] and references therein). However, the fact that the vortex may induce a magnetization distribution in the magnetic film has so far been neglected, and these theories are therefore not applicable to soft magnetic films. The aim of the current paper is to take the first step towards a theory which can explain the interactions between superconducting and soft magnetic films.

The thickness of available bismuth-substituted ferrite garnet films is today typically > 500 nm. Here we will only analyze the case of magnetic films much thinner than the superconducting penetration depth. This is clearly not justified for current garnet films, but

should be of interest in order to gain some basic understanding of the system. Moreover, in a previous paper it was proposed theoretically that reducing the thickness of the magneto-optic film is of importance when optimizing the magneto-optic image [20]. Therefore, we argue that our theory applies to thin films utilizing the Kerr effect, where all the polarization rotation takes place within the first few nanometers of the film. Kerr films may very well be a key element in future magneto-optic imaging, in particular if suitable films with high magneto-optic sensitivity and low domain activity can be found.

II. THE THIN FILM SYSTEM

Consider a thin superconducting film of infinite extent, located at $z=0$ with thickness d much smaller than the penetration depth of the superconductor. The surface is covered by an uniaxial soft magnetic film with thickness comparable to or smaller than that of the superconducting film. That is, we assume that the magnetic film consists of surface charges separated from the superconductor by a very thin oxide layer (of thickness t) to avoid spin diffusion and proximity effects. In general, the current density is a sum of the supercurrents and magnetically induced currents, which can be expressed through the generalized London equation as [17]

$$\mathbf{r} \quad \mathbf{J} = -\frac{1}{2} \frac{c}{4\pi} \nabla \times \mathbf{H} + \frac{1}{2} \nabla V(\mathbf{r}) \times \hat{\mathbf{z}} + \mathbf{r} \quad \mathbf{M}_V; \quad (1)$$

where \mathbf{J} is the current density, λ is the penetration depth, \mathbf{H} is the magnetic field and $\mathbf{r} \quad \mathbf{M}_V$ is the magnetically induced current. Note that the magnetically induced currents are included as the last term on the right-hand side of Eq. 1, and are therefore generated in the same plane as the vortex. This is justified since we assume that the thicknesses of both the superconducting and magnetic films are smaller than the penetration depth, and the magnetic film is located very close to the superconductor. The vortex is aligned in the z direction, and its source function $V(\mathbf{r})$ is assumed to be rotationally symmetric. In the case of a Pearl vortex we may set $V(\mathbf{r}) = \frac{\Phi_0}{2} \ln(r/r_0)$, where Φ_0 is the flux quantum and r_0 the permeability of vacuum.

The magnetization \mathbf{M}_V is the sum of two different contributions, \mathbf{M}_I and \mathbf{M}_B . First, the vortex induces a magnetization \mathbf{M}_I in the magnetic film, which again gives rise to opposing currents in the superconductor. Second, there may be 'hard' micromagnetic elements, e.g.

prepatterned magnetization distributions or Bloch walls, that do not experience a significant change in their magnetization distribution M_B upon interaction with the vortex. The vortex-induced magnetization can be found by assuming that the magnetooptic film is a soft magnet consisting of a single domain with in-plane magnetization in absence of external magnetic fields. Moreover, we assume that the free energy of this domain can be expressed as a sum of the uniaxial anisotropy and the demagnetizing energy. The magnetic field from a vortex tilts the magnetization vector out of the plane, and it can be shown that for small tilt angles one has [20]

$$M_I = (M_{Ix}; M_{Iz}) = M_s \frac{M_s H_{vz}}{H_a + H_v}; \quad (2)$$

where $M_I = \frac{M_{Ix}^2 + M_{Iy}^2}{M_{Ix}^2 + M_{Iy}^2 + H_v^2}$ and M_{Iz} are the in-plane and perpendicular components of the magnetization, $H_v = \frac{H_{vx}^2 + H_{vy}^2}{H_{vx}^2 + H_{vy}^2 + H_v^2}$ and H_{vz} are the in-plane and perpendicular components of the vortex field, and M_s is the saturation magnetization of the magnetic film. $H_a = M_s - 2K_u = \mu_0 M_s$ is the so-called anisotropy field, where K_u is the anisotropy constant of the magnetic film. Here the easy axis is normal to the film surface, and we neglect the cubic anisotropy of the system, which means that the in-plane magnetization direction must be the same as that induced by the vortex field. In the current work we will also assume that the anisotropy field is much larger than the in-plane vortex field, thus allowing us to write

$$M_I = M_s \left(1; \frac{H_{vz}}{H_a} \right); \quad (3)$$

Upon using Eq. 3, we neglect the contribution from the exchange energy, which is justifiable for sufficiently large K_u or small spatial field gradients.

In order to solve the generalized London equation, we follow the method of Ref. [17] and obtain

$$H_z - 2e \frac{\partial H_z}{\partial z} = V(\mathbf{r}) + d_e (\mathbf{r} - \mathbf{r}_0 \cdot M_I)_z + d_e (\mathbf{r} - \mathbf{r}_0 \cdot M_B)_z; \quad (4)$$

We now apply the superposition principle to separate the contributions from the vortex and the 'hard' magnetic elements. It is important to note that our magnetization distributions have no volume charges. Using Eq. 3, the vortex part of Eq. 4 can be written as

$$H_{vz} - 2e \frac{\partial H_{vz}}{\partial z} = V(\mathbf{r}) - \frac{\partial^2 H_{vz}}{\partial x^2} + \frac{\partial^2 H_{vz}}{\partial y^2}; \quad \frac{\partial H_{vz}}{\partial z} = \frac{d_e M_s}{H_a}; \quad (5)$$

whereas the magnetic part is

$$H_{mz} = \frac{1}{2} \frac{\partial H_{mz}}{\partial z} = d_e (r - r_0 M_B)_z : \quad (6)$$

Here we define $H_m = \sqrt{H_{mx}^2 + H_{my}^2}$ and H_{mz} to be the radial and perpendicular components of the magnetic field induced by the 'hard' micromagnetic elements.

A . Vortex solution

In order to solve Eq. (5), we use the method of Ref. [17], and find the following z and radial components of the magnetic field:

$$H_{vz}(r; z) = \frac{1}{2} \int_0^{\infty} k V(k) \frac{J_0(kr)}{1 + 2\epsilon k^2} \exp(-k|z|) dk ; \quad (7)$$

$$H_v(r; z) = \frac{1}{2} \int_0^{\infty} k V(k) \frac{J_1(kr)}{1 + 2\epsilon k^2} \exp(-k|z|) dk : \quad (8)$$

In the case $\epsilon = 0$ and $V(k) = 1$, the field is reduced to that of the standard Pearl solution [17, 22]. We also notice that there is a divergency in k -space when $1 + 2\epsilon k^2 = 0$. This is due to the fact that we assumed a very thin superconductor ($d \ll \lambda$). The divergency will therefore smooth out upon solving the London equation for arbitrary thicknesses d , but this task is outside the scope of the current work. Nonetheless, it is seen that at small distances (large k) the magnetic field may change sign as compared to the standard Pearl solution, and this is attributed to the magnetically induced currents. On the other hand, at large distances (small k) the field is basically not influenced by the soft magnetic film. A typical scale for the crossover is $k = H_a/M_s d$. One can therefore not expect to reveal this phenomenon by magneto-optic imaging, since the length scales are typically much smaller than the wavelength of light.

B . Interactions

It is of considerable interest to find the interaction between a micromagnetic element with perpendicular magnetization $M_B \hat{e}_z(z)$ and a vortex. To this end, it should be noted that the magnetic induction in the magnetic film is given by $B_I = \mu_0 (H_v + M_I)$. Here the

interaction energy between the vortex and the magnetization is given by

$$E_{vm} = \int_0^{\infty} \int_0^{2\pi} \int_0^{\infty} \mathbf{M}_B \cdot \mathbf{B} d^3r = \int_0^{\infty} \int_0^{2\pi} \int_0^{\infty} M_B \hat{e}_z (H_v + M_I) d^3r ; \quad (9)$$

where the vortex is assumed to be displaced a distance r_0 from the origin. It is clear that the radial component of the vortex-induced magnetization does not interact with M_B , since the two vectors are perpendicular to each other. However, M_B does interact with the z-component of the vortex induced field, and we find

$$E_{vm} = \int_0^{\infty} \int_0^{2\pi} \int_0^{\infty} \left(1 + \frac{M_s}{H_a} \right) M_B H_{vz} d^3r : \quad (10)$$

Equation 10 can be transformed by using the following formula:

$$\int_0^{\infty} \int_0^{2\pi} \int_0^{\infty} A(r) B(r) d^3r = \frac{1}{(2\pi)^2} \int_0^{\infty} \int_0^{2\pi} \int_0^{\infty} A(k) B(k) d^3k : \quad (11)$$

Then, in the cylindrically symmetric situation one finds

$$E_{vm} = \frac{0}{2} \int_0^{\infty} \left(1 + \frac{M_s}{H_a} \right) k V(k) \frac{M_B(k) J_0(k r_0)}{1 + 2 e^{-k}} dk : \quad (12)$$

The associated force can be found by taking the derivative with respect to r_0 , resulting in

$$F_{vm} = \frac{0}{2} \int_0^{\infty} \left(1 + \frac{M_s}{H_a} \right) k^2 V(k) \frac{M_B(k) J_1(k r_0)}{1 + 2 e^{-k}} dk : \quad (13)$$

At small distances (large k) the force may change sign due to the magnetically induced currents. Let us now assume that $M_B(k) = M_0$, i.e. that the magnetization distribution can be represented by a delta function, in order to gain some insight into this phenomenon. Then, for a Pearl vortex, the force becomes

$$F_{vm} = \frac{0 M_0}{2} \int_0^{\infty} \left(1 + \frac{M_s}{H_a} \right) k^2 \frac{J_1(k r_0)}{1 + 2 e^{-k}} dk : \quad (14)$$

When the distance is small (still larger than the coherence length ξ), we may approximate the force by

$$F_{vm} = \frac{0 M_0}{2} \int_0^{\infty} \left(1 + \frac{M_s}{H_a} \right) ; \quad < \quad \frac{M_s d}{H_a} : \quad (15)$$

Surprisingly, we see that the force is repulsive, which can be explained by the magnetically induced currents, which generate a magnetic field that opposes that produced by the vortex. For comparison, we note that in the case of an infinitely thin superconductor ($\xi = 0$) the force between a magnetic element and the vortex is at small distances approximated by

$$F_{vm} = \frac{0 M_0}{4 e^2} \int_0^{\infty} \left(1 + \frac{M_s}{H_a} \right) ; \quad < \quad e ; \quad (16)$$

which is attractive. Attractive behavior also takes place at larger distances $\rho_0 \gg \rho_e$. Then the term containing ρ_e becomes unimportant, and the force is therefore always attractive. It is interesting to note that the force is enhanced by a factor $1 + M_s/H_a$ due to the vortex-induced magnetization distribution. Therefore it should be possible to tune the interaction by changing the uniaxial anisotropy of the magneto-optic film.

In a previous work we showed that the interaction between Bloch walls and vortices in bulk superconductors are enhanced due to the image charges generated in the superconducting substrate[10]. The enhancement proposed in the current work has clearly a different origin.

III. INTERACTION WITH BLOCH WALLS

Magneto-optic films usually contain up to several nearly one dimensional domain walls (in the sense that the magnetization within the wall only varies with the x-coordinate), and these can interact with the superconductor. The 180° Bloch wall is quite common in garnet films, and also in very thin Kerr films studied here, although Neel walls may also occur in thin films if the demagnetization energy is significant. Neglecting the demagnetization energy, the magnetization vector distribution within a Bloch wall is given by[21]

$$\mathbf{M}^{\text{Bloch}} = M_s (\cos \theta; \sin \theta) ; \quad \theta = 2 \tan^{-1} \exp \left(\frac{K_u}{A} x \right) ; \quad (17)$$

where A is the exchange parameter. In addition to naturally occurring domain walls, it is also possible to pattern the magneto-optic film by depositing thin nanomagnets on its surface. Here we will model a Bloch wall using the following two different simple models with only a z component:

$$\begin{aligned} M_z^G &= M_s \exp(-x^2) \hat{e}_z ; \\ M_z^S &= \begin{cases} M_s \exp(-x^2) \hat{e}_z & \text{if } |x| < W \\ 0 & \text{if } |x| > W \end{cases} ; \end{aligned} \quad (18)$$

where we assume that $W = \frac{P}{2} = \frac{A}{2K_u}$. Using the method of Ref. [17], we find that the Gaussian magnetization distribution results in the following field components:

$$H_z^G(x; z) = \frac{e d M_s}{4\pi} \int_0^{\infty} k_x^2 \frac{\exp(-k_x^2 z^2) \cos(k_x x)}{1 + 2 e k_x} \exp(-k_x |z|) dk_x ; \quad (19)$$

$$H_x^G(x; z) = \frac{e d M_s}{4\pi} \int_0^{\infty} k_x^2 \frac{\exp(-k_x^2 z^2) \sin(k_x x)}{1 + 2 e k_x} \exp(-k_x |z|) dk_x ; \quad (20)$$

On the other hand, the step magnetization distribution gives

$$H_z^S(\mathbf{x};z) = \frac{2e d M_s}{0} \int_0^{Z/2} k_x \frac{\sin(k_x W) \cos(k_x x)}{1 + 2e k_x} \exp(-k_x |z|) dk_x ; \quad (21)$$

$$H_x^S(\mathbf{x};z) = \frac{2e d M_s}{0} \int_0^{Z/2} k_x \frac{\sin(k_x W) \sin(k_x x)}{1 + 2e k_x} \exp(-k_x |z|) dk_x : \quad (22)$$

Figure 1 shows H_z^G (solid line) and H_x^G (dash-dotted line) for $e = 40W$ and $z = 0$. As expected, the H_z^G is symmetric about the origin and has its maximum field here, whereas H_x^G is zero at $x = 0$. Note also that H_x^G changes sign at $x = 0$, and has peaks at $x = \pm 0.02$. Figure 2 shows H_z^G (solid line) and H_z^S (dash-dotted line) for $e = 40W$ and $z = e = 200$. Note that in contrast to H_z^G , H_z^S has two peaks at the edges of the magnetization distribution. Thus, it is seen that these two magnetization distributions give rise to different characteristic features which may be resolved by magneto-optic imaging.

The force between the one dimensional magnetization distribution and a Pearl vortex is found to be

$$F(x) = -\frac{0}{1 + \frac{M_s}{H_a}} \int_0^{Z/2} k_x \frac{M(k_x) \sin(k_x x)}{1 + 2e k_x} \frac{1}{k_x^2} dk_x : \quad (23)$$

If the Bloch wall is represented by a Gaussian magnetization distribution, the interaction force is found from Eq. 23 to be

$$F(x) = -\frac{M_s}{1 + \frac{M_s}{H_a}} \int_0^{Z/2} k_x \frac{\exp(-k_x^2/4) \sin(k_x x)}{1 + 2e k_x} \frac{1}{k_x^2} dk_x : \quad (24)$$

Fig. 3 shows the interaction force in the limit $d \rightarrow 0$. The solid line corresponds to $H_a = 0.2M_s$ and the dash-dotted line to $H_a = 0.5M_s$. It is seen that the force is always attractive.

IV. MAGNETO-OPTIC IMAGING OF BLOCH WALLS

A powerful property of magneto-optic films is that they can visualize the vortices and Bloch walls simultaneously, thus allowing us to study the dynamics of these elements. However, it is difficult to draw conclusions about the field from the Bloch wall based on a single magneto-optic film, unless the width of the wall is altered by the superconductor[0]. On the other hand, it is of considerable interest to study the structure of the Bloch wall in presence of the superconducting film in order to gain additional information about the interaction between such systems. This can be done by placing a second magneto-optic

indicator above our thin InS system (composed of a thin superconducting and magneto-optic In). However, care must be taken, since the signal detected by the polarization microscope depends on the gap l between the thin In system and the second indicator. Moreover, let us assume that the second indicator has thickness D , and does not interact with the thin In system. A model for magneto-optic imaging was introduced in Ref. [20], and this will be used here (neglecting absorption). Figures 4 and 5 show the signal modulation for Gaussian and step-like magnetization distributions using two different indicators. In Fig. 4 a very thin indicator ($D = W/2$, $\epsilon = 40W$) positioned close to the thin In structure ($l = W/10$) is used. We see that the characteristic magnetic field profiles can be revealed. However, in Fig. 5 a thicker indicator ($D = 2W$, $\epsilon = 40W$) and a larger gap l ($l = W/5$) is assumed. Although the signal profile generated by the Gaussian distribution does not change much, it is seen that the characteristic peaks from the step like distribution are lost. Thus, we conclude that a small gap and a thin indicator is necessary to reveal the characteristic magnetic field profiles discussed above. It should be pointed out that vortices may also be present, thus changing the detected signal. However, a study of this effect is outside the scope of the current work.

V. CONCLUSION

We have studied the interaction between magneto-optic and superconducting InS . It was shown that the vortex induces a magnetization distribution in the magneto-optic In , thus modifying the magnetic field as well as the interaction Bloch walls. In particular, we show that by tuning the anisotropy field of the magneto-optic In , one may enhance this interaction. We also discussed some simple implications for magneto-optic imaging.

Acknowledgments

The author is grateful to H. Hauglin, P. E. Goa, M. Bazilevich, T. H. Johansen and E. I. Il'yashenko for many interesting discussions on this topic, and also to T. M. Fischer for generous support.

-
- [1] P.B. Ablers, Phys. Rev. 105, 104 (1957).
 - [2] H. Kirschner Phys. Lett. A 26A, 651 (1968).
 - [3] H.J. Habermeyer and H. Kronmüller, Appl. Phys. 12, 297 (1977).
 - [4] L.A. Dorosinskii, M.V. Indenbom, V.I. Nikitenko, Y.A. Ossip'yan, A.A. Polyanskii and V.K. Vlasov, Physica C 203, 149 (1992).
 - [5] C. Jooss, R. Warthmann and H. Kronmüller, Phys. Rev. B, 61, 12433 (2000).
 - [6] M.R. Koblischka and R.J. Wijngaarden, Supercond. Sci. Technol. 199, 8 (1995).
 - [7] M.R. Koblischka, T.H. Johansen, H. Bratsberg, and P. Vase, Supercond. Sci. Technol. 11, 573 (1998).
 - [8] T.H. Johansen, M. Bazilevich, H. Bratsberg, Y. Galperin, P.E. Lindolf, Y. Shen and P. Vase, Phys. Rev. B, 54, 16264 (1996).
 - [9] A.A. Polyanskii, X.Y. Cai, D.M. Feldmann and D.C. Larbalestier, NATO Science Series, Vol. 3/72, p.353, Kluwer Academic Publishers, Dordrecht, 1999.
 - [10] L.E. Helseth, P.E. Goa, H. Hauglin, M. Bazilevich and T.H. Johansen, Phys. Rev. B, 65, 132514 (2002).
 - [11] L.E. Helseth, A.G. Solov'yev, R.W. Hansen, E.I. Il'yashenko, M. Bazilevich and T.H. Johansen, Phys. Rev. B 66, 064405 (2002).
 - [12] M. Shamoon, M. Klink, O. Hagedorn and H. Dotsch Appl. Opt. 40, 3182 (2001).
 - [13] C. Jooss, J. Albrecht, H. Kuhn, S. Leonhardt, and H. Kronmüller, Rep. Prog. Phys. 65, 651 (2002).
 - [14] P.E. Goa, H. Hauglin, M. Bazilevich, E.I. Il'yashenko, P.L. Gammel and T.H. Johansen, Supercond. Sci. Technol. 14, 729 (2001).
 - [15] P.E. Goa, H. Hauglin, A.A.F. Olsen, M. Bazilevich and T.H. Johansen, Rev. Sci. Instrum. 74, 141 (2003).
 - [16] P.E. Goa, H. Hauglin, A.A.F. Olsen, D.V. Shantsev and T.H. Johansen, Appl. Phys. Lett. 82, 79 (2003).
 - [17] L.E. Helseth, Phys. Rev. B 66, 104508 (2002).
 - [18] S. Erdin, A.F. Kayali, I.F. Lyuksyov and V.L. Pokrovsky, Phys. Rev. B 66, 014414 (2002).
 - [19] M.V. Milosevic, S.V. Yampolskii and F.M. Peeters, Phys. Rev. B 66, 174519 (2002).

- [20] L.E. Helseth, J. Magn. Magn. Mat. 247, 230 (2002).
- [21] D. Craik, 'Magnetism : Principles and Applications', John Wiley & Sons, Chichester, 1995.
- [22] J. Pearl, Appl. Phys. Lett. 5, 65 (1964).

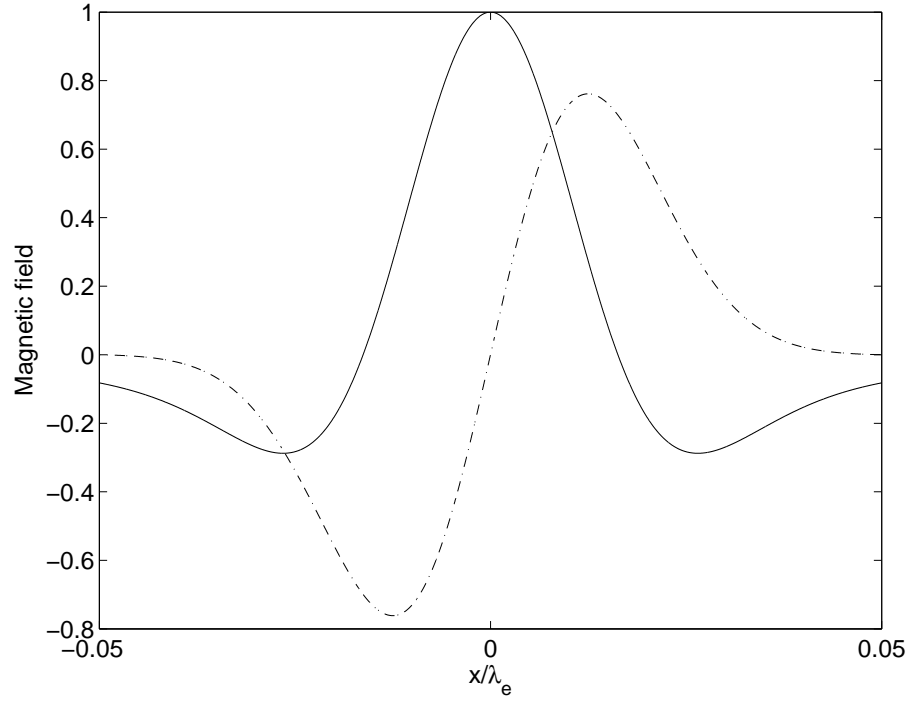


FIG .1: The x (dash-dotted line) and z (solid line) component of the magnetic field generated by a gaussian magnetization distribution. Here $z=0$ and $W = \lambda_e=40$. The curves are normalized with respect to the maximum peak of the z component.

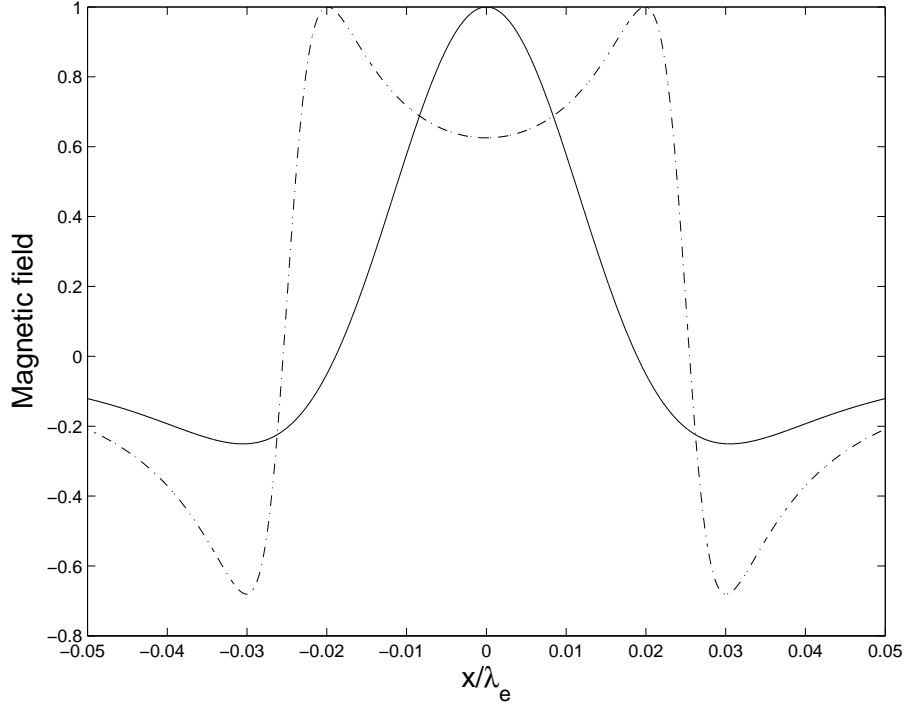


FIG . 2: The z components of the magnetic field generated by gaussian (solid line) and step-like (dash-dotted line) magnetization distributions. Here $z = z_e = 200$ and $W = W_e = 40$. The curves are normalized with respect to the maximum peak of each of the z components.

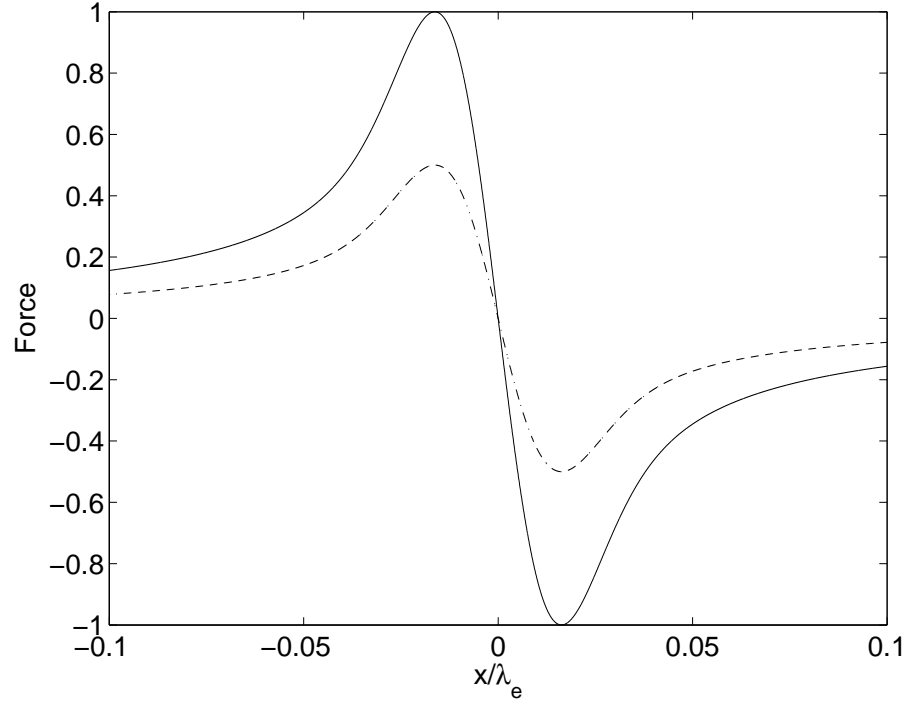


FIG . 3: The normalized interaction force for a gaussian magnetization distribution when $\mu_e = \frac{p}{3200}$. The solid line corresponds to $H_a = 0.2M_s$, and the dash-dotted line to $H_a = 0.5M_s$.

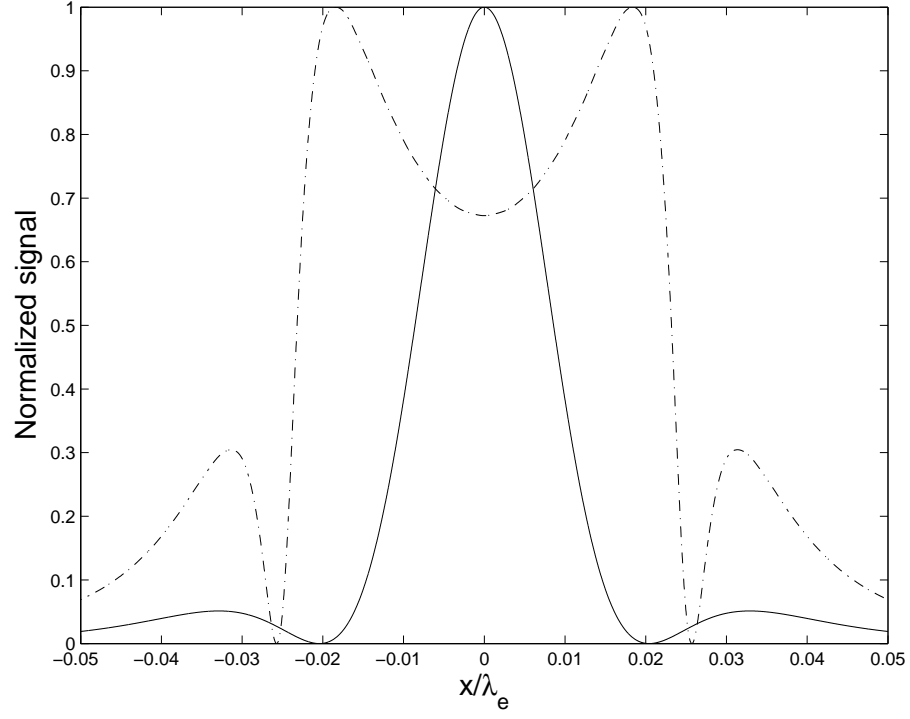


FIG . 4: The normalized signal as a function of position for a gaussian (solid line) and step-like (dash-dotted line) magnetization distribution. Here we have chosen $W = \lambda_e = 40$, $l = W/10$ and $D = W/2$.

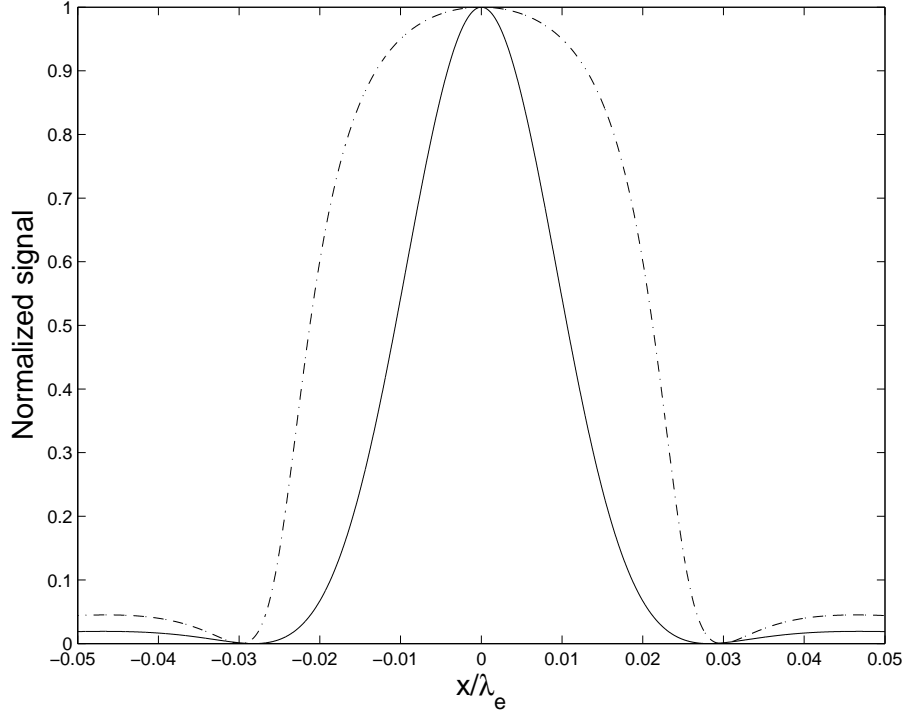


FIG . 5: The normalized signal as a function of position for a gaussian (solid line) and step-like (dash-dotted line) magnetization distribution. Here we have chosen $W = \lambda_e/40$, $l = W/5$ and $D = 2W$.